ARID ZONE JOURNAL OF ENGINEERING, TECHNOLOGY & ENVIRONMENT
AZOJETE September 2023. Vol. 19(3):447-460
Published by the Faculty of Engineering, University of Maiduguri, Maiduguri, Nigeria.
Print ISSN: 1596-2490, Electronic ISSN: 2545-5818
www.azojete.com.ng

ORIGINAL RESEARCH ARTICLE

THE EFFECTS OF ATMOSPHERIC ATTENUATIONS ON C, KU AND KA FREQUENCY BANDS ON SATELLITE COMMUNICATION SYSTEM

E. U. Udo, O. A. Nwaorgu, K. O. Odo* and N. D. Kanu

Department of Electrical and Electronic Engineering, Michael Okpara University of Agriculture, Umudike, Abia State.
**Corresponding author's email address: kayceebby@yahoo.co.uk*

ARTICLE INFORMATION

Submitted 2 March, 2023
Revised 2 May, 2023
Accepted 7 May, 2023

Keywords:
Atmospheric attenuation
Rain attenuation
Fuzzy logic
Satellite communication

ABSTRACT

This paper presents the effects of atmospheric attenuations on C, Ku and Ka microwave frequency bands. The atmospheric attenuations such as cloud, rain, oxygen and water vapour have a much significant effect on the transmitting and receiving of signals over satellite communication especially in locations prone to rainfall. This paper analyzed the effects of atmospheric attenuation on satellite communications in selected location in the city of Aba. The rainfall, cloud and gas data were measured and collected from the Nigerian meteorological agency for a period of three months using simulink model to determine the frequency bands within the areas affected by bad weather condition. The method employed the use of Matlab and International telecommunication union radiocommunication sector (ITU-R) prediction model which include the fuzzy logic system to improve the received signal on satellite communication. The results obtained shows that for the exceedance time of 0.01, the attenuation values recorded during the rainfall at elevation angles of 10^0, 20^0, 30^0 and 40^0 are 14.0440, 17.84080, 25.32430, 13.45070, 17.67230, 24.05440, 14.37360, 18.35890, 26.18720, 13.12440, 16.62090, 23.31440, 12.70280, 16.03920 and 22.36270 while for the exceedance time of 1.00, the attenuation values recorded are 0.639130, 0.88553, 1.41930, 0.605330, 0.834540, 1.32490, 0.62090, 0.91320, 1.48480, 0.585040, 0.804960, 1.26970, 0.560440, 0.767250 and 1.2080 respectively. Therefore, the work reported here showed that the effects of satellite connection which suffers from poor signal quality due to atmospheric disturbances in the study area was minimized.

1.0 Introduction

Satellite communications are essentially used for providing communication links between different areas on the earth by receiving information from a transmitting earth station. Satellite communications play an important role globally in the telecommunications system. About 3,000 satellites are orbiting the earth relaying continuous and discrete information bearing data, video and audio from one location to another in the world. Satellite based communication networks at high frequencies are rapidly expanding. These high frequency operations have enabled a large number of available applications and services including communications, navigation, telemedicine, remote sensing, network sensors distribution and access to internet without the use of wires. However, high frequency applications can generally result to large transmission problems because of atmospheric attenuations (Harb et al., 2012).

Satellite communications that operate at high frequencies beyond 10 GHz are expected to deliver a wider bandwidth and a higher data rate for multimedia and broadband services. However, such systems have to cope with strong atmospheric impairments, mainly due to rain. This particular impairment is even worse in the tropical regions, which are mostly characterized by heavy

precipitation. In this case, deep signal fading due to rain will definitely affect the quality of analogue transmissions and increase the error rate of digital transmissions, (Idrissa et al, 2016).

A satellite functions most effectively if the transmissions are directed to a desired area. When the desired area of coverage is focused, the emissions do not move away from the designated area and it minimizes the interference to the other systems. Without a functioning communication link, most satellites are rendered useless. To ensure a proper satellite to ground link, one has to make estimations of the signal attenuation because of the distance to the satellite, atmospheric distortions and other system specific losses. An important aspect is noise originating in the system components and from general background radiation ((Vangli, 2010).

The effect of atmosphere is a primary issue when designing satellite-to-earth links operating at frequencies beyond 10 GHz. Droplets of rain absorb and scatter radio waves, leading to signal attenuation and decrease in the system reliability and availability. It also causes one of the major fundamental problems on the communication satellite links performance, resulting to large variations in the signal power at the receiver end. (Osahenvemwen and Omoriguwa, 2017). However, satellite services using 10GHz frequencies and above are influenced by different propagation impairments like attenuation caused by rain, cloud and ice depolarization (Osahenvemwen and Omoriguwa, 2013).

Interestingly, There are some basic effects of propagation abnormalities which affect the communication satellite systems performance. In a satellite communication, weather losses result from degradation of the satellite signals by hydrometers as they cross the earth's atmosphere. Some of the losses encountered by satellite communication systems are rain, cloud and gas attenuations. When higher frequencies are transmitted and received under heavy attenuations, signal degradation which is proportional to the intensity of propagation abnormalities occurs.

The radio frequency in Ka band offers three advantages for satellite communication over the low frequencies of C and Ku bands in terms of spectrum availability, reduced interference potential and reduced equipment size. Satellite signals inevitably confront propagation impairments during signal transmissions between the satellite and earth stations. The Ka band is more susceptible to tropospheric impairments than lower frequencies which can degrade service quality. Rain, ice, fog, gas, clouds and moist air affect communication links in different ways. If estimation of such impairments can be done, proper mitigation techniques can be implemented to improve the quality of service (Sujimol et al., 2015).

Attenuation caused by rain, cloud and gas are primary sources of impairment to information propagation at millimeter and microwave wavebands. These impairments become particularly severe at higher frequencies, especially beyond Ku-band. Therefore, it is very difficult to maximally utilize satellite based network resources which are affected by weather attenuations (Singh et al., 2017).

Ishag et al., (2015) carried out a design and implementation of attenuation due to rain control and reduce simulation modules in MATLAB simulator in order to investigate the Ku band signal

Corresponding author's e-mail address: kayceebby@yahoo.co.uk

efficiency under the rain attenuation effect. The results showed that the horizontally polarized signal was more attenuated by the rain than the circularly and vertically polarized signal.

Ajewole et al., (2017) investigated rain effects on the performance of Ku-band satellite signals in Akure, Nigeria. Comparison of the predicted rain induced attenuation estimated by applying the measured data was conducted with some chosen rain attenuation models like ITU-R, Garcia and Moupfouma. The results showed that the time series of rainfall during a typical rainy event is the reception pattern at Ku-band. This is an indication that there is a very strong relationship between the reduction of the satellite signals and the rate of rainfall recorded. However, they did not consider worst cases of rain rates above 120mm/hr that could help to improve the efficiency of the results.

Osahenvemwen and Omorogiuwa, (2017) described in a study that attenuation increases as rainfall rate increases and the vertical polarized signal offers less rain attenuation than the horizontal polarized signal at Ku and Ka bands.

Furthermore, Odo et al., (2021) conducted a comparative analysis of rain attenuation models in satellite links and discovered that rain attenuation is a major source of impairment to signal propagation at microwave and millimeter wavebands. Also, rain attenuation causes a distorting effect on signal quality at higher frequencies leading to digital transmission errors. The knowledge of rain attenuation and its performance was essential in order to optimize system capacity. The authors used ITU-R, DAH and Ajayi models for estimating rain attenuation. Therefore our research focused on the effects of performance improvement of satellite communication over atmospheric attenuations on C, Ku and Ka frequency bands for proper implementation of the attenuation model in the satellite communication and the selection of the frequency band that best suite transmission.

2. Materials and methods

The materials used in this study include coaxial cable**,** rain gauge**,** stopwatch**,** compass**,** radiosonde**,** parabolic reflector antenna**,** Matlab/Simulink and PC.

Data was obtained from the Nigerian meteorological agency for a period of three months and analyzed in Matlab/Simulink. The models were implemented based on the International Telecommunication Union radio wave sector recommendations considered to be suitable for satellite communications (ITU-R 2017).

The general satellite system model contains three main components, viz; earth stations, satellites and the links between the channels. The channel and receiver models were created using MATLAB/SIMULINK.

The city of Aba in Abia state of Nigeria was chosen as a study area to investigate satellite attenuation and how atmospheric condition affects satellite communication with different bands in the area. Atmospheric condition of these areas such as rainfall rate, rain height above sea level, and liquid water content of rain drops, temperature and relative humidity were taken into consideration.

Corresponding author's e-mail address: kayceebby@yahoo.co.uk

The effect of raindrops was determined at higher transmission frequencies, especially above 10 – 250 GHz. The effects of how other atmospheric phenomena such as clouds, water vapour and oxygen causes signal attenuation was discovered.

2.1 Mathematical modeling of the rain attenuation model

The rain attenuation model shown in figure 1 was implemented based on the modified ITU-R prediction model. The model includes the fuzzy logic inference system which acts as a decision scheme to select and adjust the satellite connection to most bands that favors certain weather impairment within the selected location. The initialization includes values for earth station position parameters of latitude and altitude above sea level, rain parameters such as rain rate, rain height and percentage of exceeding time p and transmitter parameters of frequency f, elevation angle θ and polarization angle τ.

The developed Simulink model performs two procedures simultaneously. The first method starts by obtaining the frequency-dependent rain damping empirical values before calculating the rain-specific coefficients r and ε as shown in equations (1) and (2).

$$r = \frac{r_H + r_V + (r_H - r_V)Cos^2\theta Cos2\tau}{2} \quad (1)$$

$$\varepsilon = \frac{r_H\varepsilon_h + r_v\varepsilon_v + (r_H\varepsilon_H - r_v\varepsilon_v)cos^2\theta\cos(2\tau)}{2k} \quad (2)$$

The rain-specific attenuation (the rain attenuation per 1 km) is then calculated using equation (3) dependent on the actual measured precipitation rate (at p = 0.01%)

$$\delta_{Rain} = \varepsilon(R_{0.01})^k \quad (3)$$

This value will be applied in the second method to identify the effective path length as well as to predict the overall rain attenuation. The horizontal reduction factor (r_H) for 0.01% at the time can be calculated using equation (4).

$$r_H = \frac{1}{1+0.78\sqrt{\frac{P_H\delta_R}{f}} - 0.38\left(1-e^{-2P_H}\right)} \quad (4)$$

where P_H is the horizontal projection which depends on the slant path length and the elevation angle as shown in equation (5).

$$P_H = S_L\cos\theta \quad (5)$$

The slant path length depends on the vertical height from the earth station to the rain height as well as on θ, as shown in equation (6).

$$S_L = \begin{cases} \frac{H_R - H_S}{\sin\theta} & for\ \theta \geq 5° \\ \frac{2(H_R - H_S)}{\sqrt{sin^2\theta + \frac{2(H_R - H_S)}{E_R}} + \sin\theta} & for\theta \geq 5° \end{cases} \quad (6)$$

Corresponding author's e-mail address: kayceebby@yahoo.co.uk

where H_R and H_s are the rain and earth station heights above sea level and E_R is the earth radius. The vertical change factor (V_F) can be calculated at 0.01% of the time using equations (7) to (8).

$$\omega = \tan^{-1}\left(\frac{H_R - H_S}{P_H r_H}\right) \quad (7)$$

$$R_L = \begin{cases} \frac{P_H r_H}{\cos\theta} & for\ \omega > \theta \\ \frac{H_R - H_S}{\sin\theta} & for \omega \geq 5° \end{cases} \quad (8)$$

$$V_F = \frac{1}{1+\sqrt{\sin\theta}\left[31\left(1-e^{\frac{\theta}{1-x}}\right)\frac{\sqrt{R_L\delta_R}}{f^2}-0.45\right]} \quad (9)$$

Where x depends on the latitude (φ) of the earth station. The effective path length can be obtained using equation (10), whereas the total rain attenuation at 0.01% of time ($A_{0.01}$) can be calculated using equation (11) (Fiebig et al., 2004).

$$E_L = R_L V_F \quad (10)$$

$$A_{0.01} = E_L \delta_R \quad (11)$$

Consequently, the predicted rain attenuation at any percentage of time (p) can be calculated using equations (12) and (13).

$$\begin{cases} 0 & if\ p \geq 1\%\ or\ |\varphi| \geq 36° \\ -0.005(|\varphi| - 36) & if\ p < 1\%\ and\ |\varphi| < 36°\ and\ \theta \geq 25° \\ -0.005(|\varphi| - 36) + 1.8 - 4.25sin\theta & otherwise \end{cases} \quad (12)$$

$$A_{rain} = A_{0.01}\left(\frac{p}{0.01}\right)^{-[0.655+0.033\ln(p)-0.045ln(A_{0.01})-\beta(1-p)sin\theta]} \quad (13)$$

2.2 Mathematical modeling of the cloud attenuation

The amount of liquid water content contained in the cloud is also responsible for absorption and scattering of electromagnetic energy especially for frequencies above 10 GHz but with less intensity than that of rain. Cloud attenuation in addition to the transmission parameters (signal frequency, elevation angle) rests on the cloud parameters such as average height and thickness, total columnar content of liquid water and temperature (Singh et al., 2017). However, the cloud specific attenuation coefficient can be calculated using equation (14).

$$\delta_{cloud} = \frac{0.819f}{e^{"}\left[1-\left(\frac{2+e'}{e^{"}}\right)^2\right]} \quad (14)$$

The cloud attenuation at any probability depends on the liquid water content that can be obtained from radiometric measurements for the selected regions as shown in equation (15).

$$A_{cloud} = \delta_{cloud}\left(\frac{LWC}{sin\theta}\right) \quad (15)\ \text{(ITU-2002).}$$

Figure 1 describes the block diagram of the cloud attenuation process used to calculate liquid water content and temperature.

Corresponding author's e-mail address: kayceebby@yahoo.co.uk

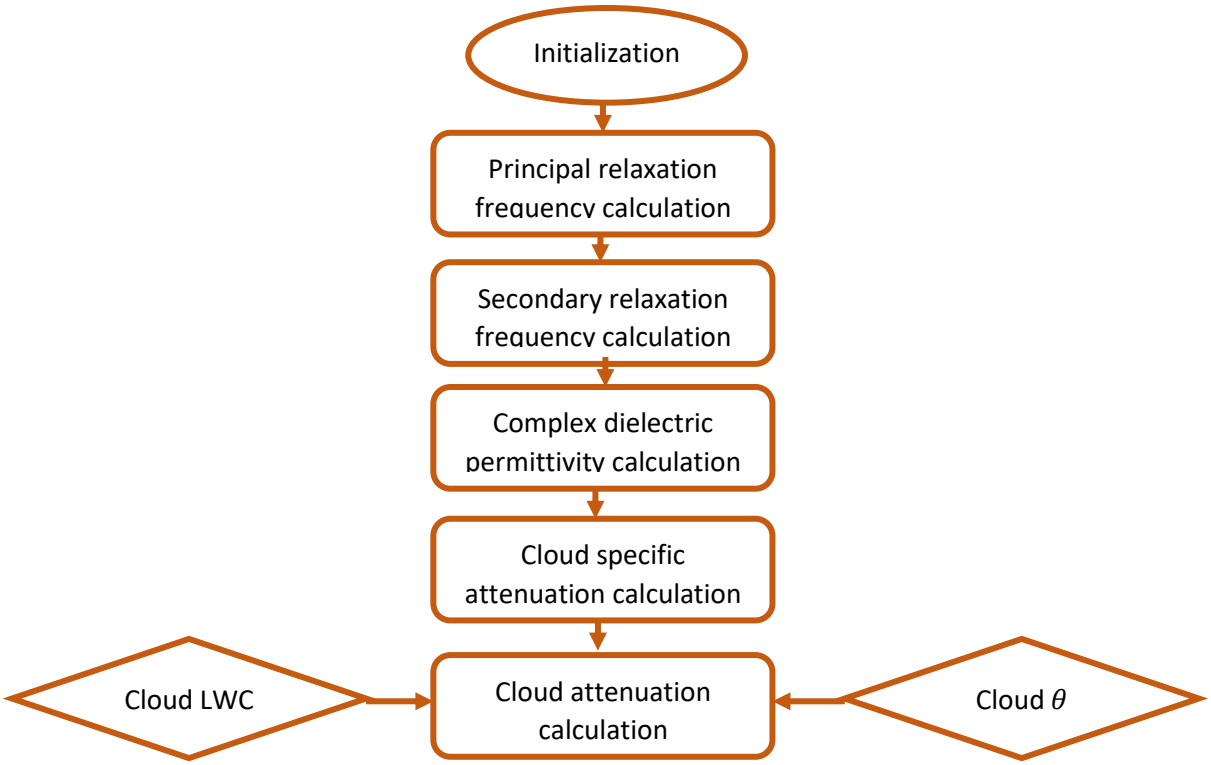

Figure 1: Cloud attenuation model

2.3 Water vapor and oxygen attenuations models

The effective water vapour path length is based on the assumption of an exponential atmosphere to describe the relation between water vapour density and altitude. The water vapour specific attenuation in (dB/km) can be calculated as shown in equation (16).

$$\delta_w = f^2 r_T^{2.5} \rho [s_1 + s_3 + s_4 + s_5 + s_6 + s_7 + s_8 + s_9] \times 10^{-4} \quad (16)$$

The total gas attenuation A_{Gases} for oxygen and water vapour attenuations can be predicted using equation (17).

$$A_{Gases} = \frac{A_o + A_W}{sin\theta} = \frac{\gamma_O L_O + \gamma_W L_W}{sin\theta} \quad (17)$$ (Al-Samawi et al., 2022).

2.4 Simulink implementation of the rain attenuation model

The rain attenuation model used in this paper is obtained from the ITU-R standard rain attenuation. The Simulink used for the rain attenuation model was attached directly to the fuzzy logic decision making for selection of parameter. The Simulink implementation of the rain attenuation model is shown in figure 2.

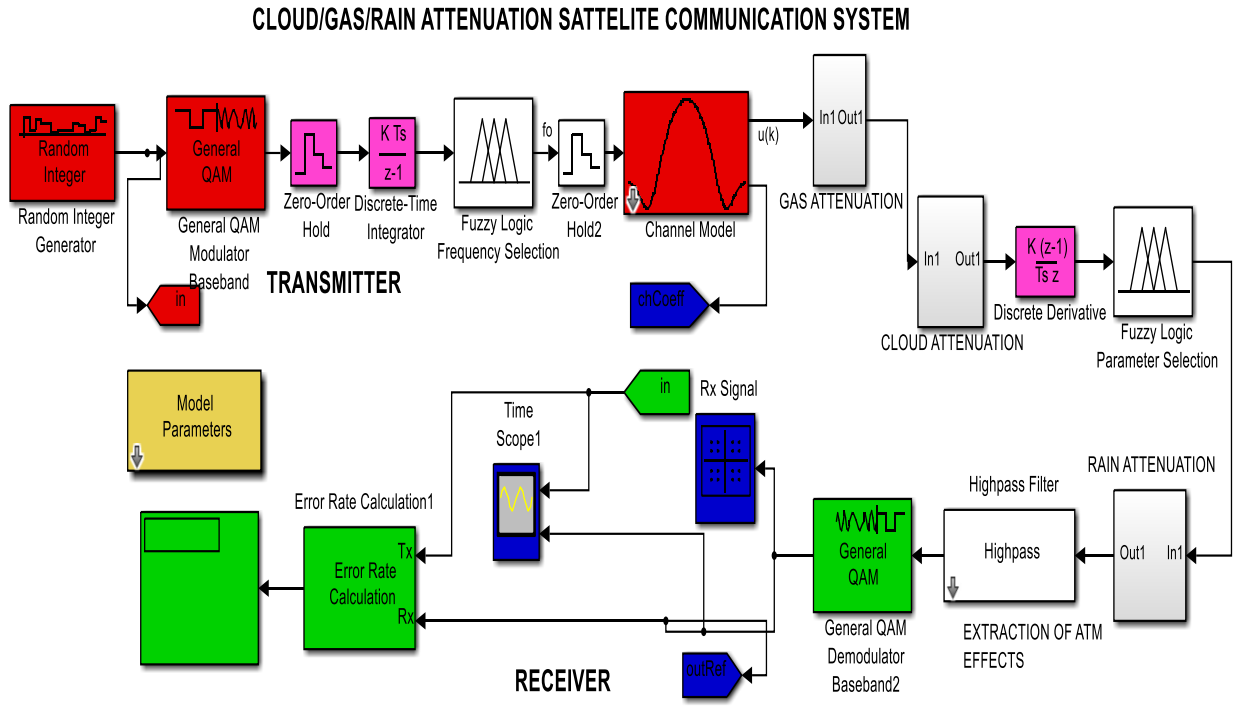

Figure 2: Simulink implementation of the satellite communication system with attenuation model

3. Results and Discussion

The percentage of exceedance time for rain attenuation was tabulated from 0.01 to 1.00 for various elevation angles of 10, 20, 30, 40 and 50 degrees for C, Ku and Ka bands. Table 1 shows the rain attenuation values at various frequency bands for different elevation angle. The results revealed that, the higher the elevation angle, the lower the attenuation and therefore the higher the values of Eb/No. I*t* was also observed that, bad weather attenuates satellite transmission to a large extent in the study area. This is because during heavy rainfall, bad channel quality imposes serious problems to the users of the satellite network. This leads to communication link outage at lower elevation angles θ. The elevation angle depends on the Eb/No along with the transmission bit rate and bandwidth.

Corresponding author's e-mail address: kayceebby@yahoo.co.uk

Table 1: Rain attenuation values at C, Ku and Ka bands at different elevation angles

	@ Elevation angle =10 degree			@ Elevation angle =20 degree			@ Elevation angle =30 degree			@ Elevation angle =40 degree			@ Elevation angle =50 degree		
Percentage of exceedance time	C	Ku	Ka	C	Ku	Ka	C	Ku	Ka	C	Ku	Ka	C	Ku	Ka
0.01	14.0440	17.84080	25.32430	13.45070	17.67230	24.05440	14.37360	18.35890	26.18720	13.12440	16.62090	23.31440	12.70280	16.03920	22.36270
0.020	12.45470	16.050	22.9940	11.94060	15.29210	21.80480	12.8050	16.48620	23.80840	11.64880	14.87390	21.1110	11.26180	14.33560	20.22430
0.030	11.46380	14.8060	21.41860	10.98610	14.12870	20.28690	11.78530	15.25440	22.18190	10.70510	13.73480	19.6290	10.34250	13.22810	18.78860
0.040	10.73580	13.90920	20.23080	10.28250	13.26930	19.14760	11.04110	14.34170	20.9690	10.01590	12.89440	18.51830	9.67210	12.41240	17.71490
0.050	10.16450	13.20490	19.28180	9.73090	12.59120	18.2390	10.45670	13.61980	19.99290	9.4760	12.23180	17.63330	9.14740	11.79510	16.86040
0.060	9.69650	12.62480	18.49390	9.27940	12.03320	17.48550	9.97750	13.02480	19.18190	9.03430	11.68680	16.90	8.71840	11.24170	16.15310
0.070	9.30140	12.13310	17.8820	8.89860	11.56060	16.84340	9.5730	12.52040	18.48970	8.66190	11.22560	16.27550	8.35690	10.79510	15.55130
0.080	8.96080	11.70760	17.23740	8.57830	11.15190	16.28530	9.22390	12.08360	17.88720	8.3410	10.82670	15.7330	8.04550	10.40910	15.02870
0.090	8.66180	11.33340	16.72090	8.28240	10.79260	15.79260	8.91770	11.69930	17.35480	8.05970	10.47630	15.25410	7.77270	9.76820	14.56770
0.010	8.39630	11	16.25910	8.02680	10.47270	15.35230	8.65540	11.35690	16.87850	7.80990	10.16430	14.82640	7.53030	7.84510	14.15610
0.020	6.71150	8.86710	13.26730	6.40720	8.42490	12.50490	6.9170	9.1640	13.78870	6.22870	8.17330	12.06340	5.9990	6.79200	11.50140
0.030	5.79450	7.69340	11.59350	5.52720	7.30690	10.91590	5.97510	7.95560	12.05740	5.37060	7.08120	10.52380	5.16910	6.08550	10.02510
0.040	5.18160	6.90380	10.45640	4.93970	6.55280	9.83790	5.34510	7.1420	10.880	4.7980	6.34790	9.48030	4.61590	5.56290	9.02560
0.050	4.72950	6.31850	9.60760	4.50670	5.99430	9.03410	4.88020	6.53860	10.050	4.37620	5.80520	8.70260	4.20850	5.15320	8.28140
0.060	4.37570	5.85880	8.93710	4.1680	5.55590	8.39970	4.51620	6.06450	9.30550	4.04640	5.37930	8.08920	3.89020	4.81900	7.69470
0.070	4.08760	5.48340	8.38720	3.89240	5.19180	7.87970	4.21970	5.67720	8.73520	3.77810	5.03190	7.58650	3.63140	4.53870	7.21430
0.080	3.84640	5.16820	7.92560	3.66170	4.89790	7.44160	3.97140	5.35180	8.25420	3.55360	4.74030	7.16320	3.41480	4.29860	6.80990
0.090	3.640	4.89780	7.52470	3.46440	4.64040	7.06480	3.75890	5.07270	7.84020	3.36160	4.49050	6.79930	3.22970	4.08940	6.46230
0.10	3.46040	4.66210	7.17590	3.29270	4.41460	6.73550	3.57390	4.82930	7.47810	3.19470	4.27280	6.48130	3.06880	3.83300	6.15870
0.20	2.39480	3.25380	5.06960	2.27560	3.06740	4.74990	2.47560	3.37380	5.28930	2.20590	2.97470	4.56570	2.11660	2.84350	4.33220
0.30	1.86050	2.54030	3.98630	1.76640	2.4040	3.73110	1.92530	2.63560	4.16190	1.71150	2.31910	3.58410	1.64110	2.21520	3.39790
0.40	1.5190	2.08140	3.28260	1.44140	1.96550	3.07020	1.57170	2.16030	3.42890	1.39610	1.89820	2.94790	1.3380	1.81220	2.79310
0.50	1.27570	1.7520	2.77410	1.20950	1.65370	2.5930	1.31980	1.81910	2.89880	1.17110	1.59660	2.48890	1.1220	1.52370	2.35710
0.60	1.08970	1.5050	2.38350	1.03320	1.41570	2.22690	1.12180	1.55830	2.49140	1.020	1.36650	1.85590	0.957960	1.30360	2.02290

Corresponding author's e-mail address: kayceebby@yahoo.co.uk

0.70	0.947740	1.3050	2.07150	0.893530	1.22660	1.93460	0.976160	1.3510	2.16580	0.864850	1.18370	1.85560	0.828120	1.12900	1.75640
0.80	0.822940	1.13170	1.81540	0.779780	1.07220	1.69490	0.852270	1.040	1.89850	0.754620	1.03450	1.62560	0.722420	0.986420	1.53800
0.90	0.72330	1.090	1.60120	0.68520	0.943460	1.49440	0.749190	0.920330	1.67480	0.662990	0.910150	1.43310	0.634570	0.867670	1.35550
1.00	0.639130	0.88553	1.41930	0.605330	0.834540	1.32490	0.62090	0.91320	1.48480	0.585040	0.804960	1.26970	0.560440	0.767250	1.2080

Continuation of rain attenuation values at C, Ku and Ka bands at different elevation angles

Corresponding author's e-mail address: kayceebby@yahoo.co.uk

Figures 3 to 7 showed that the higher the percentage of exceedance time, the lower the attenuation. Similarly, for the given elevation angle of rainy weather events, the higher the attenuation, the lower the elevation angle, the higher the rain Eb/No. It means that the increase in attenuation at lower elevation angle will affect the signal-to-noise ratio in satellite communication.

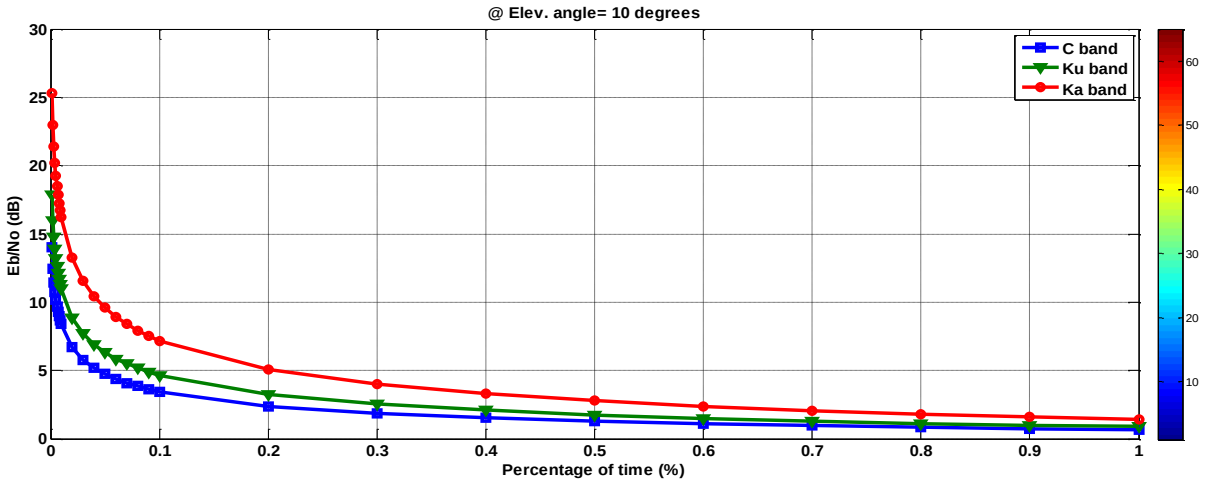

Figure 3: Graph of percentage of time (%) against signal – to – noise ratio (Eb/No) for C, Ku and Ka frequency bands at 10° elevation angle

The graph of Eb/No with rainfall events for C, Ku and Ka frequency bands at 10° elevation angle is shown in figure 3. It is observed that the values of Eb/No at 0.1 percentage of exceedance time are 4 dB, 5 dB and 7.5 dB respectively. It is an indication that an increase in the percentage of exceedance will lower the attenuation.

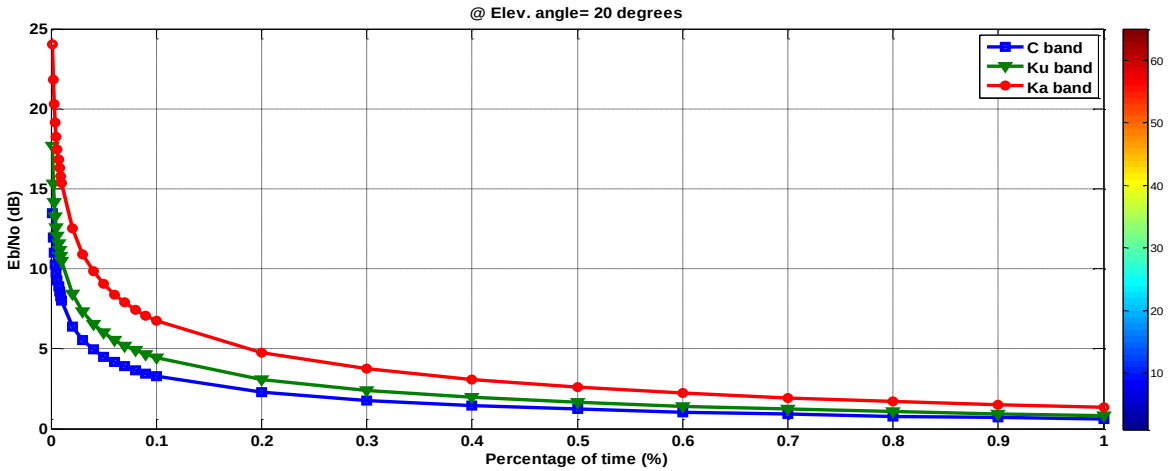

Figure 4: Graph of percentage of time against signal – to – noise ratio for C, Ku and Ka frequency bands at 20° elevation angle

The graph of Eb/No with rainfall events for C, Ku and Ka frequency bands at 20° elevation angle is shown in figure 4. It is observed that the values of Eb/No at 0.1 percentage of exceedance time are 3 dB, 4.5 dB and 7 dB respectively. This indicates that an increase in the percentage of exceedance will lower the attenuation.

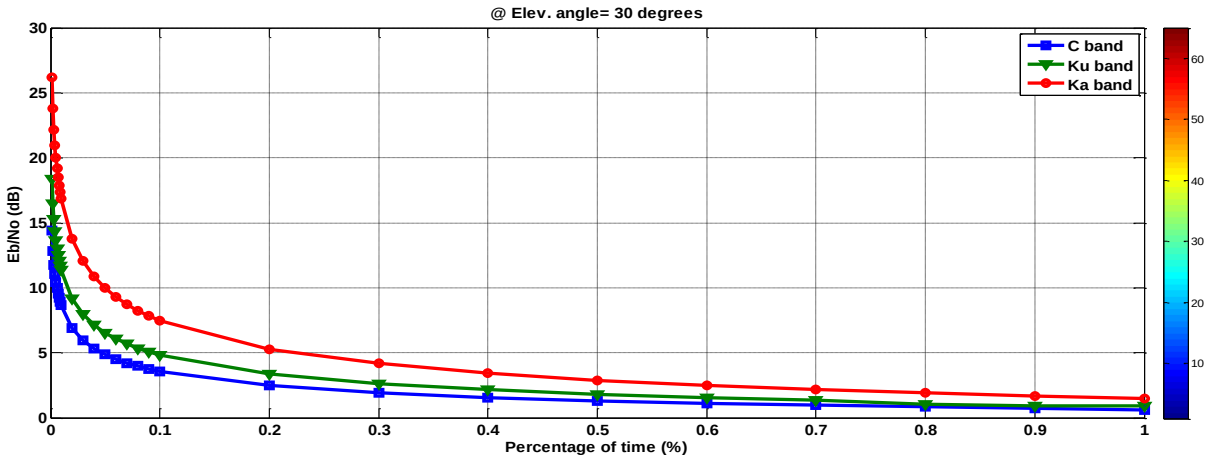

Figure 5: Graph of percentage of time against signal-to-noise ratio for C, Ku and Ka frequency bands at 30° elevation angle

The graph of Eb/No with rainfall events for C, Ku and Ka frequency bands at 30° elevation angle is shown in figure 5. It is seen that the values of Eb/No at 0.1 percentage of exceedance time are 4 dB, 5 dB and 8 dB respectively. It is an indication that an increase in the percentage of exceedance will lower the attenuation.

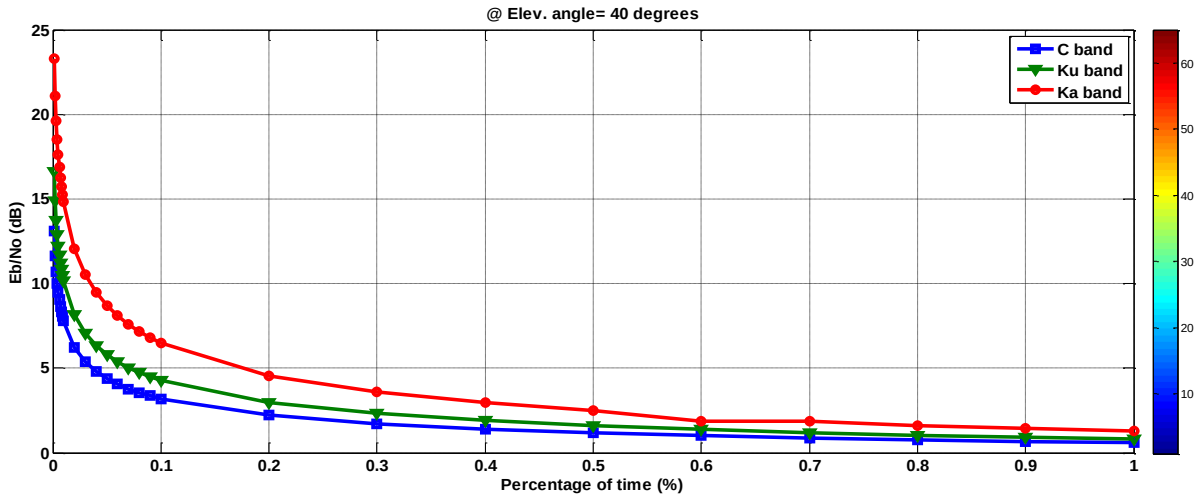

Figure 6: Graph of percentage of time against signal-to-noise ratio for C, Ku and Ka frequency bands at 40° elevation angle

The graph of Eb/No with rainfall events for C, Ku and Ka frequency bands at 40° elevation angle is shown in figure 6. It is seen that the values of Eb/No at 0.1 percentage of exceedance time are 3 dB, 4.5 dB and 6 dB respectively. It indicates that an increase in the percentage of exceedance will lower the attenuation.

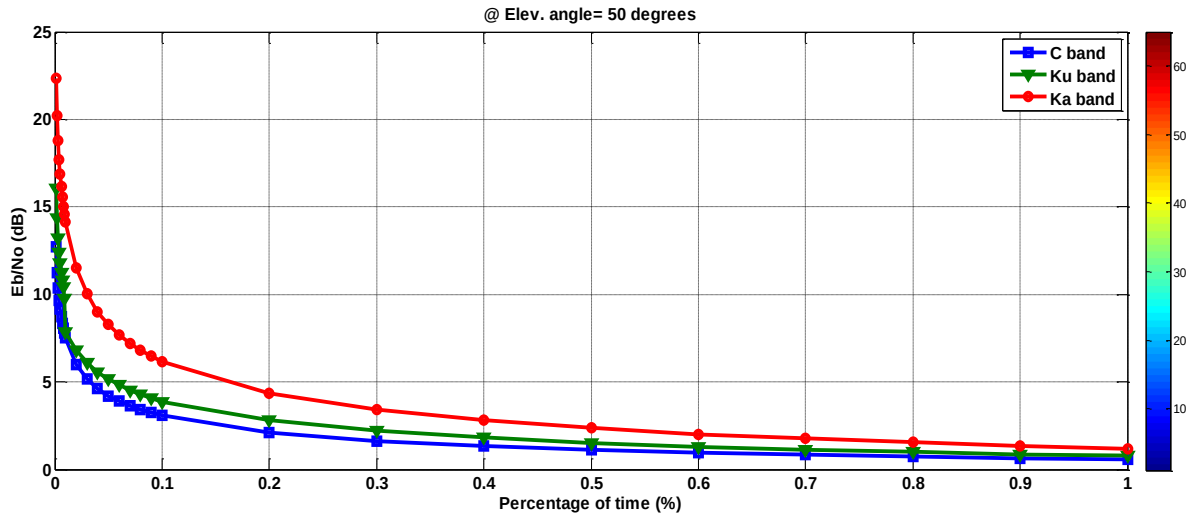

Figure 7: Graph of percentage of time against signal-to-noise ratio for C, Ku and Ka frequency bands at 50° elevation angle

The graph of Eb/No with rainfall events for C, Ku and Ka frequency bands at 50° elevation angle is shown in figure 7. It is observed that the values of Eb/No at 0.1 percentage of exceedance time are 3 dB, 4 dB and 6 dB respectively. It is an indication that an increase in the percentage of exceedance will lower the attenuation.

3.1 Gas attenuation

The significant amount of dry air and water vapour attenuation appears at specific regions across the frequency spectrum. across The asynchronous transfer mode of the selected locations in Aba and the total correlated gases attenuation at various relative humidity's are shown in figure 8. The gas attenuation was seen to increase as frequency increases from 250 GHz for a significant increase in relative humidity of the gases.

The specific gas attenuation started at frequencies above 100 GHz due to the effect of oxygen before the attenuation level went down. The effect appeared again at frequencies above 210, 310 and 410 GHz during selection by the fuzzy logic inference system. This effect occurs due to water vapour attenuation and to select the best frequency using fuzzy logic band at the expense of weather with varying relative humidity.

Corresponding author's e-mail address: kayceebby@yahoo.co.uk

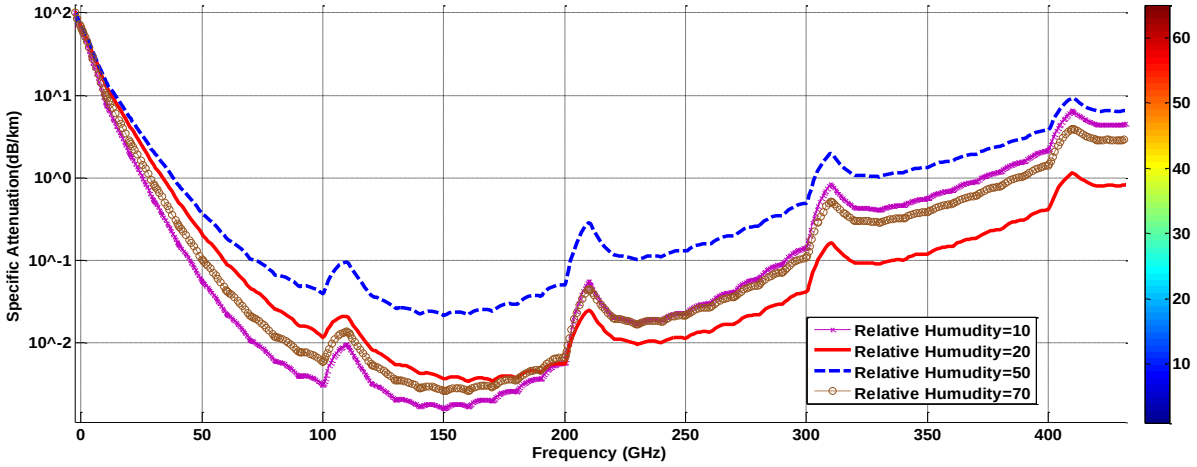

Figure 8: Gas attenuation at various relative humidity

4. Conclusion

This paper presented the effects of atmospheric impairments and its attenuation effects to the satellite signal quality in terms of performance evaluation and assessments concerning various effective atmospheric and transmission parameters during dynamic weather conditions. The models for cloud, gas and rain attenuation were developed based on ITU-R standard and these models were implemented using Matlab/simulink.

The gases attenuation at fixed 50% relative humility reached higher level at approximately 415 GHz. The relative humidity is directly proportional to the amount of signal power attenuation due to the water vapour particles in space, and the total gases attenuation.

However, the location such as Ogbor hill and Umungansi in the study area usually suffer from higher relative humility which indicates increased gas attenuation in the location, so proper implementation of the attenuation model in the satellite communication will help initiate the selection of the frequency band that best suite transmission.

The plots of attenuation against the percentage of exceedance time decreases at various rainfall events of C, Ku and Ka frequency bands at $10°C, 20°C, 30°C, 40°C$ and $50°C$ and these indicates that an increase in the percentage of exceedance lowers the attenuation signal.

References

Abubakar, I., Lam, HY. and Din, J. 2016. Implementation of adaptive coding and modulation for satellite communication links in heavy rain region: An operator's perspective. ARPN Journal of Engineering and Applied Sciences, 11 (12): 7858-7861.

Al-Saegh, AM., Sali, A., Ismail, A. and Mandeep, JS. 2014. Analysis and modeling of the cloud impairments of satellite-to-land mobile channel at Ku and Ka bands. 7th Advanced Satellite Multimedia Systems Conference and the 13th Signal Processing for Space Communications Workshop, 436–441. doi.org/10.1109/ASMS-SPSC.2014.6934579

Corresponding author's e-mail address: kayceebby@yahoo.co.uk

Ajewole, MO., Durodola, OM. and Ojo, JS. 2017. Performance of ku-band satellite signals received during rainy condition in two low latitude tropical locations of Nigeria. Adamawa State University Journal of Scientific Research, 1(5): 1-17.

Harb, K., Yu, FR. and Abdul-Jauwad, S. 2012. Performance evolution in satellite communication networks along markovian channel prediction. Journal of Wireless Networking and Communications, 2(5): 143-157.

Fiebig, U., Sigliar, R., Heder, B. and Csurgai, L. 2004. Comparison of rain attenuation models of satellite communication channels based on measured point rain intensity. International Conference on Telecommunications and Computer Networks, 1: 837- 843.

ITU, 2002. "Handbook on Satellite Communications," 3rd Edition, Wiley, New York.

Jang, JS. 1997. A course in fuzzy systems and control. Prentice Hall, Upper Saddle River, New Jersey, pp 424.

ITU-R, 2017. Propagation data and prediction methods required for the design of earth-space telecommunication systems. ITU Radiocommunication Assembly, Jeneva, 1-28. ITU-R P.618-13.

Odo, KO., Okoro, CK., Iroegbu, C. and Ogbonnaya, IJ. 2021. Comparative analysis of rain attenuation models in satellite links. Journal of Engineering and Applied Sciences, 19(1): 494 – 505.

Osahenvemwen, OA. and Omorogiuwa, O. 2013. Effect of Rain on Satellite Communication Networks in Nigeria: Case Study of Warri Town, Journal of Nigeria Association of Mathematical Physics, 25(2): 107-114. (http://nampjournals.org/abstracts/vol25abstract.pdf)

Osahenvemwen, OA. and Omorogiuwa, O. 2017. Rain attenuation analysis from system operating at Ka and Ku frequency bands. American Journal of Advanced Research, 1: 7-12.

Singh, H., Kumar, R., Bonev, B. and Petkov, P. 2017. Cloud attenuation issues in satellite communications at millimeter frequency bands-state of art. International Journal of Scientific and Engineering Research, 8(7): 858–862.

Sujimol, MR., Acharya, R., Singh, G. and Gupta, RK. 2015. Rain attenuation using ka and ku band frequency beacons at delhi earth station. Indian Journal of Radio and Space Physics, 44: 45-50

Corresponding author's e-mail address: kayceebby@yahoo.co.uk